ACS OMEGA

http://pubs.acs.org/journal/acsodf

Article

Multilayer Structure Ammoniated Collagen Fibers for Fast Adsorption of Anionic Dyes

Wei Luo, Ruiyang Chi, Fanke Zeng, Yahan Wu, Yun Chen, Shuting Liu, Wei Lin, Huiting Lin, Xiaoxia Ye,* and Jie Chen*

Cite This: *ACS Omega* 2021, 6, 27070−27079

Read Online

ACCESS | Metrics & More | Article Recommendations | Supporting Information

ABSTRACT: Dye wastewater has become one of the difficult industrial wastewaters due to its significant characteristics such as high chroma and poor biodegradability. Here, we use collagen fibers (CFs) as the matrix, glutaraldehyde as the cross-linking agent, and polyethyleneimine (PEI) as the ammoniating modifier to prepare cationic-modified collagen fibers (CF-PEI). The CF-PEI still maintained the original fibrous structure with a larger adsorption area. The content of primary amino groups on CF-PEI was significantly increased, which not only improved the hydrophilic swelling performance of CFs but also improved the adsorption capacity. The adsorption capacity of CF-PEI for soap yellow and acid red could reach 538.2 and 369.7 mg g^{-1}, respectively. The adsorption rate was fast, and the adsorption equilibrium could be reached in about 60 min. Desorption regeneration studies have shown that 0.1 mol L^{-1} HCl could achieve a better desorption effect, and the CF-PEI had a good recycling performance. The ammoniated modified CF-PEI was an excellent adsorption treatment material for anionic dye wastewater. It is expected to become an effective way for high-value resource utilization of waste dander in the leather industry.

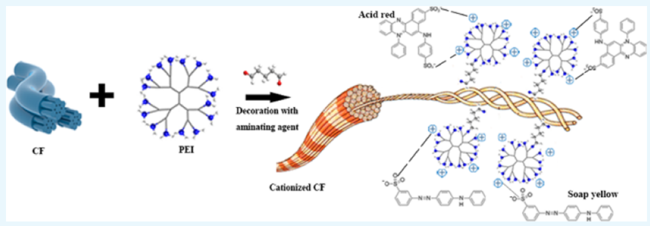

1. INTRODUCTION

Dyes are organic compounds that can color fibers or other substances and are widely used in various industries.[1−4] However, most dyes are highly toxic and are difficult to biodegrade. Therefore, the removal of dyes in industrial wastewater is one of the important research contents in the field of environmental protection.[5,6] The most commonly used method to treat dye wastewater is adsorption.[7−10] However, traditional adsorbents, such as activated carbon[11−14] and resins,[15,16] have problems such as difficult elution, loss of adsorbents, and high energy consumption when adsorbing dyes, which fail to achieve harmless treatment of dye wastewater. At present, there are many types of dyestuffs in common use, among which the anionic dyestuffs are the most widely used because of their rich variety, complete color, and good dyeing effect.[17,18] Therefore, the development of adsorbents to remove anionic dyestuffs in water has a wide range of application value and prospects.

In the tanning industry, the utilization rate of raw leather is low, only 30−50% of them can be converted into useable leather, and the rest is mainly in the form of waste leather shavings.[19−21] Therefore, a large amount of waste leather shavings is produced every year. At present, except for a small part of the waste leather shavings used to produce recycled leather and to prepare gelatin, most of the remaining shavings are treated as garbage, which causes a very serious waste of resources. How to reuse waste dander is also a hot issue in the tanning industry. Skin collagen fibers (CFs) extracted from waste leather shavings are white short fibrous solids, which are hydrophilic and insoluble in water and become dispersed after swelling in water.[22,23] Skin CFs are structural proteins, and the amino acids that constitute collagen are rich in active groups such as −COOH, $-NH_2$, and −OH.[24−27] In addition, type I collagen, the main component of CFs, has a characteristic three-helix structure. The above-mentioned characteristics and structure indicate that skin CFs are a potential adsorbent material. At the same time, it is cheap, nontoxic, harmless, and biodegradable and can also be used as a new type of biomass material. According to fiber morphology, CFs can be divided into nonfibrous CFs and fibrous CFs.[28,29] The CF extracted from the waste leather dander through acid, alkali, and enzyme treatments is a natural linear polymer. Its amino acid composition is very close to that of the human skin. It has a high affinity and is biodegradable. This kind of "green" fiber can be widely used in various fields. At present, the utilization of CFs is mainly divided into two categories. One is based on the unique macroscopic properties of CFs, that is, fiber

Received: July 10, 2021
Accepted: September 24, 2021
Published: October 5, 2021

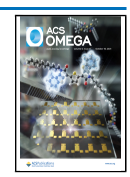

Scheme 1. Chemical Formula for Acid Red (a) and Soap Yellow (b)

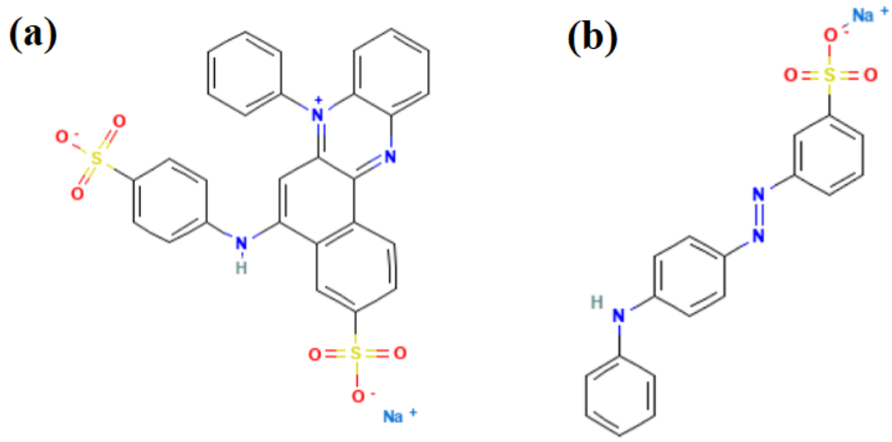

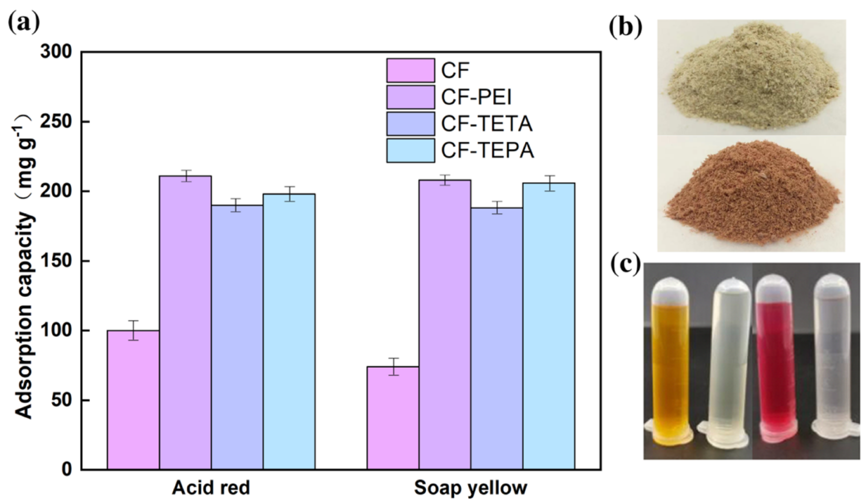

Figure 1. (a) Adsorption properties of three kinds of ammoniated CFs for anionic dyes, (b) digital pictures of CF and CF-PEI, and (c) digital images of soap yellow(left) and acid red (right) before and after adsorption by CF-PEI.

properties, which are used in the fields of photographic paper, papermaking, textiles, and so forth. The second is based on its good properties of biocompatibility, biodegradability, and low antigenicity which can be widely used in food,[30] cosmetics,[31] biomedical materials,[32] drug slow-release,[33] tissue engineering materials,[34] chemical raw materials,[35] wastewater treatment,[36,37] and other fields. The current research on CF materials is still mainly focused on theoretical and semi-practical aspects, such as material manufacturing methods, physics and chemistry, and simulation performance.[38−40] Although many valuable results have been achieved, there is still a considerable distance from industrial application. Therefore, it is necessary to further broaden its application fields on the basis of the original theoretical research and application.

Herein, CFs with the characteristics of expanding and dispersing in water and being hydrophilic and insoluble in water were used as a biomass adsorbent to treat dye wastewater, fundamentally solving the pollution problem of dyes to the environment, so as to achieve the requirements of reasonable and effective use of tanning waste and circular economy. However, the adsorption capacity of unmodified CFs for dyes is only about 30 mg g^{-1}. In order to improve the removal rate of dyes, CFs are used as raw materials and modified by amination to prepare a series of cationic CF adsorbents. By increasing the cation content on the CFs, the ability to remove anionic dyes in the water body is enhanced, and the harmful substances in the water body are separated. Different amino reagents are studied to select the most suitable one. Common anionic dyes including soap yellow ($C_{18}H_{14}N_3NaO_3S$, Scheme 1) and acid red ($C_{28}H_{18}N_3NaO_6S_2$, Scheme 1) were selected as the treatment objects, and the effects of different pH values, adsorption time, initial mass concentration of the target object, and adsorption temperature on the adsorption performance of modified CFs were investigated. The adsorption behavior of pollutants is studied through the adsorption isotherm model, adsorption thermodynamics, and adsorption kinetics. In this study, the elution effect of different desorbents was further investigated, and the repeated regeneration performance of the cationic CF was studied.

2. RESULTS AND DISCUSSION

2.1. Optimization of Preparation of Ammoniated CFs.

Three different ammoniating agent-modified CFs and unmodified CFs were used in the adsorption experiment of 100 mL of 100 mg L^{-1} simulated dye wastewater. The results are shown in Figure 1a. CF composed of structural protein is rich in active groups such as −COOH, $-NH_2$, and −OH and has a certain adsorption capacity for dyes, but the adsorption

https://doi.org/10.1021/acsomega.1c03643
ACS Omega 2021, 6, 27070−27079

capacity is low. The adsorption capacity of the three types of ammoniated modified CF for anionic dyes has been greatly improved. Among them, polyethyleneimine (PEI) has the best modification effect, so PEI is selected as an ammoniating agent for the subsequent preparation of cationized CFs.

CF-PEI was prepared by the cross-linking reaction with CF as the base, PEI as the functional group, and glutaraldehyde as the cross-linking agent. The preparation principle is shown in Figure S1. The aldehyde group at one end of the glutaraldehyde molecule reacts with the amino groups on the CF chain in the Schiff base reaction. The aldehyde group at the other end reacts with the amino group of PEI in the Schiff base reaction. The preparation conditions of CF-PEI were further optimized. The preparation reaction temperature was set to 298, 308, and 318 K; the mass ratio of PEI to CF was 1:1 for modification; 0.05 g of CF-PEI was taken to adsorb acid red and soap yellow, and the adsorption amount was measured. The CF-PEI prepared at 308 K has a better adsorption effect, so 308 K is chosen as the reaction temperature for subsequent modification preparation (Figure S2). Under these conditions, CF-PEI with a mass ratio of CF to ammoniating agent of 2:1, 1:1, and 1:2 was prepared, and adsorption experiments were performed on simulated dye wastewater to explore the best ratio of PEI and CF. When the mass ratio of CF/PEI is 1:1, the modified CF-PEI has the best adsorption performance for simulated dye wastewater (Figure S3). Therefore, the skin CF powder to PEI mass ratio of 1:1 is selected as the reactant ratio for subsequent experiments for other studies. Figure 1b,c shows the optimized CF-PEI digital photos as well as the digital photos before and after the soap yellow and acid red solutions were adsorbed by CF-PEI. CF changed from grayish white to brownish red before and after modification, indicating that PEI was successfully grafted onto CF. The dye color faded obviously before and after adsorption, indicating that the adsorption effect of CF-PEI was excellent.

2.2. Characterization of CF and CF-PEI. CF is a supramolecular structure formed by self-assembly of type I collagen molecules. As shown in Figure S4, the basic structural unit of CF is collagen fibrils with an average diameter of 50−200 nm. These nanoscale collagen fibrils self-assemble layer by layer to form micrometer fibers, and the micrometer fibers are further assembled into fiber bundles and finally assembled into a three-dimensional network structure, thereby forming CFs with a multilayer structure. The nanometer−micrometer−macro-scale multilayer structure of CF has the following characteristics: the multilayer full-fiber structure is mainly based on rapid surface mass transfer with low mass transfer resistance; the layer-by-layer self-assembled multilevel fiber structure can realize the multilevel fiber drainage effect to achieve rapid mass transfer. The scanning electron microscopy images of CF-PEI are shown in Figure 2a−d. It can be seen from Figure 2c,d that the modified CF still maintains the original fiber structure, so it can still swell, disperse, and maintain the fibrous structure when treating dye wastewater, which can ensure that the adsorption area before and after modification is basically unchanged. At the same time, it has the relevant mechanical properties of the original CF, which provides a structural guarantee for the subsequent desorption and regeneration and repeated use. The Fourier transform infrared (FT-IR) spectrum of CF-PEI is shown in Figure 2e. For CF and CF-PEI, there is a strong absorption peak at the wavenumber of 3285 cm^{-1}, which is caused by the superposition of the stretching vibration of the hydroxyl group and the primary amino group. PEI also has an absorption peak at 3285 cm^{-1}, which is due to the stretching vibration of the primary amino group. Compared with the CF, the absorption peak of CF-PEI at 3285 cm^{-1} is significantly stronger, indicating that the primary amino groups have been successfully introduced into the skin CFs. In addition, CF-PEI has an absorption peak of 2832 cm^{-1}, and the absorption peak of CF-PEI at 2935 cm^{-1} is significantly stronger than that of CF, which is caused by the asymmetric stretching vibration of the methylene group. This shows that PEI was successfully grafted onto CF through the cross-linking effect of glutaraldehyde, and a large amount of methylene was introduced, which enhanced the absorption of CF-PEI at 2935 and 2832 cm^{-1} after modification. FT-IR analysis shows that PEI was successfully grafted to CF under the cross-linking effect of glutaraldehyde. A large number of amino groups on PEI makes CF-PEI more hydrophilic and easier to contact and adsorb dye wastewater. At the same time, a large number of amino groups on PEI provide more cation adsorption sites, thereby greatly improving the CF's ability to treat anionic dye wastewater. The X-ray photoelectron spectroscopy (XPS) spectra of CF and CF-PEI before and after modification are shown in Figure S5. It can be seen that the relative content of N increased significantly after grafting PEI, which was caused by the amino group in PEI. Figure S6 shows the zeta potentials of CF-PEI and CF. Compared with CF, the zeta potential curve and isoelectric point of CF-PEI after grafting were significantly changed, and the isoelectric point changed from 6.8 to 8.2, indicating that the positively charged PEI was successfully grafted, and the isoelectric point of CF-PEI increased. Figure S7 shows the fiber morphology of CF and CF-PEI before and after water absorption. As shown in Figure S7, the swelling degree of CF is not obvious after water

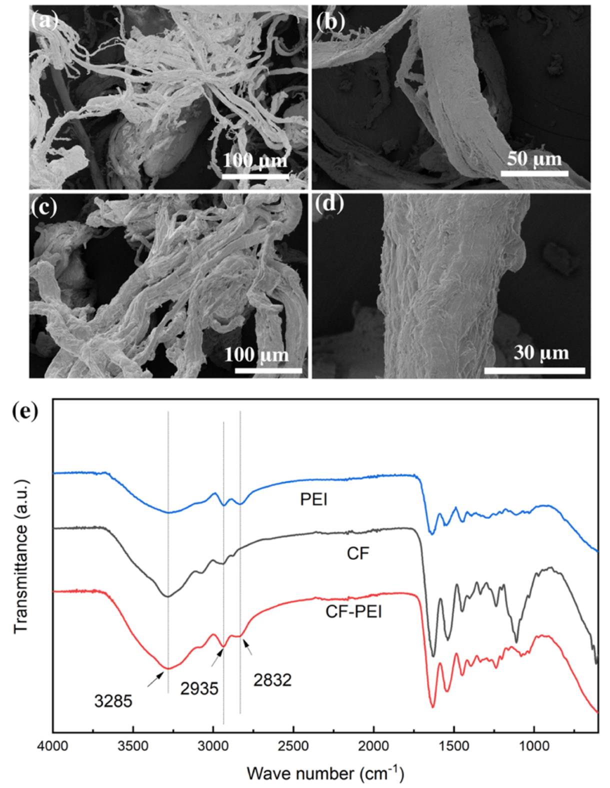

Figure 2. FESEM images of the CF (a,b) and CF-PEI (c,d). (e) FT-IR spectra of PEI, CF, and CF-PEI.

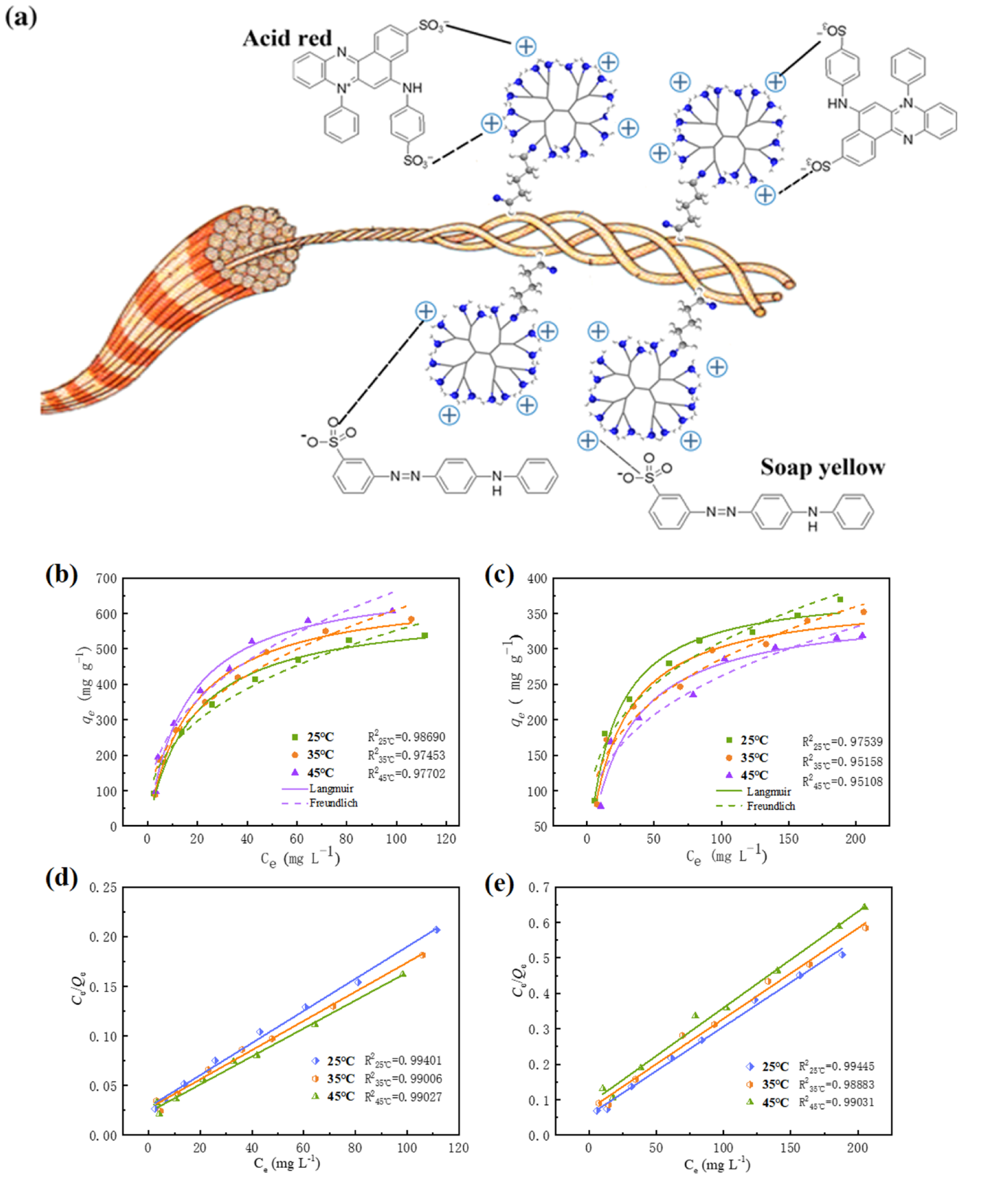

Figure 3. (a) Schematic diagram of adsorption of acid dye by CF-PEI. Adsorption isotherms of soap yellow (b) and acid red (c) adsorbed by CF-PEI and isotherms of soap yellow (d) and acid red (e) adsorbed by CF-PEI fitted by the Langmuir equation.

absorption, and the fiber is still very dense. However, the swelling degree of CF-PEI is obvious after water absorption, and the fiber diameter is significantly increased. The results showed that the hydrophilicity and swelling property of CF-PEI were improved.

2.3. Adsorption Performance. The influence of different pH values on the adsorption of simulated dye wastewater by CF-PEI is shown in Figure S8. The adsorption effects of CF-PEI on simulated dye wastewater are different under different pH conditions, and the effects on soap yellow and acid red dyes are also different. In general, the adsorption effect of CF-PEI was better in the range of pH = 3−9 for soap yellow and acid red simulated dye wastewater: the removal rate of both dyes was more than 95% and the adsorption capacity was about 200 mg g^{-1}. When pH > 9, the removal rate and adsorption capacity of CF-PEI began to decrease, and the effect of CF-PEI on acid red was more obvious. The reason is that the amino group in acidic solution binds to the proton and

https://doi.org/10.1021/acsomega.1c03643
ACS Omega 2021, 6, 27070−27079

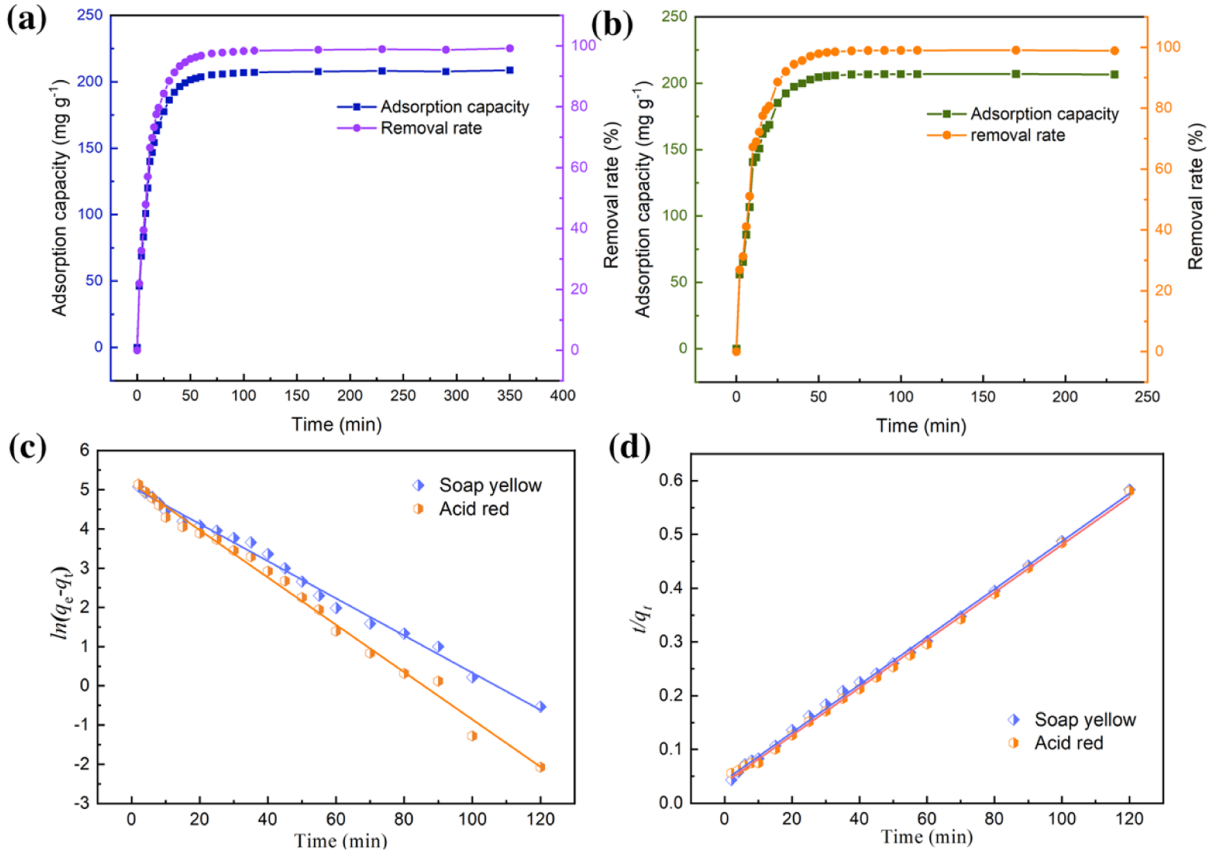

Figure 4. Kinetics of the adsorption of soap yellow (a) and acid red (b) onto CF-PEI, (c) kinetics of the adsorption fitted by the pseudo-first-order equation, and (d) kinetics of the adsorption fitted by the pseudo-second-order equation.

makes its own positive electricity increase, and then the negative electric group and the protonated amino group combine with stronger ionic bond under acidic conditions to achieve the purpose of adsorption and removal. However, hydroxide ions under alkaline conditions will affect the morphology and negative charge performance of anion dyes, which is not conducive to adsorption. Considering the adsorption capacity and removal rate of soap yellow and acid red by CF-PEI at different pH values, pH = 4 was selected as the best adsorption pH for soap yellow and pH = 7 was selected as the best adsorption pH for acid red.

The XPS spectra of CF-PEI and CF-PEI after adsorbing soap yellow and acid red are shown in Figure S9. The original CF-PEI mainly contains C, N, and O elements. After adsorption of soap yellow and acid red, a characteristic peak of S 2p appeared at a binding energy of 165 eV. The XPS spectrum analysis showed that soap yellow and acid red were successfully adsorbed by CF-PEI. Figure 3a shows the adsorption mechanism of CF-PEI on soap yellow and acid red. The adsorption isotherms of acid red and soap yellow by CF-PEI are shown in Figure 3b,c. As can be seen from Figure 3b,c, in the range of low dye concentration, the removal rate gradually increases with the increase of dye concentration. When the concentration of soap was 150 mg L^{-1}, the maximum removal rate was 95.1%. The maximum removal rate of acid red was 93.6% at 100 mg L^{-1}. When the initial dye concentration reached a certain range, the removal rate decreased with the increase of the initial dye concentration. The reason for this phenomenon is that when the initial mass concentration of dye is high, the adsorption sites of CF-PEI are limited, and the adsorption tends to be saturated, which will prevent the adsorption from continuing, thus resulting in a decrease in the removal rate. The equilibrium adsorption capacity of CF-PEI on soap yellow and acid red increased with the increase of the initial dye mass concentration. When the initial dye mass concentration was increased from 50 to 400 mg L^{-1}, the equilibrium adsorption capacity of CF-PEI on soap yellow and acid red increased from 92.2 and 85.9 mg g^{-1} to 538.2 and 369.7 mg g^{-1}, respectively. This is because the higher the initial mass concentration, the higher the mass transfer force between the solution and the surface of CF-PEI and the higher the probability of collision between dye molecules and the surface of the adsorbent, so that the adsorption capacity of CF-PEI increases. Within the set temperature range, the temperature rise had different effects on the adsorption effect of CF-PEI adsorbent on soap yellow and acid red. The adsorption capacity and removal rate of CF-PEI increased with the increase of temperature, which indicated that the adsorption process was endothermic. The maximum adsorption capacity was 194.1 mg g^{-1} and the maximum removal rate was 98.0% at 318 K. However, the adsorption effect of CF-PEI on acid red decreased with the increase of temperature, indicating that the adsorption process was exothermic. At 298 K, the maximum adsorption capacity was 180.3 mg g^{-1} and the maximum removal rate was 93.6%. Generally speaking, the adsorption capacity was within the temperature range of room temperature and higher than room temperature. The temperature has little effect on the equilibrium adsorption capacity of soap yellow and acid red (<5% from 298 to 318 K), and the removal rate is also at a

https://doi.org/10.1021/acsomega.1c03643
ACS Omega 2021, 6, 27070−27079

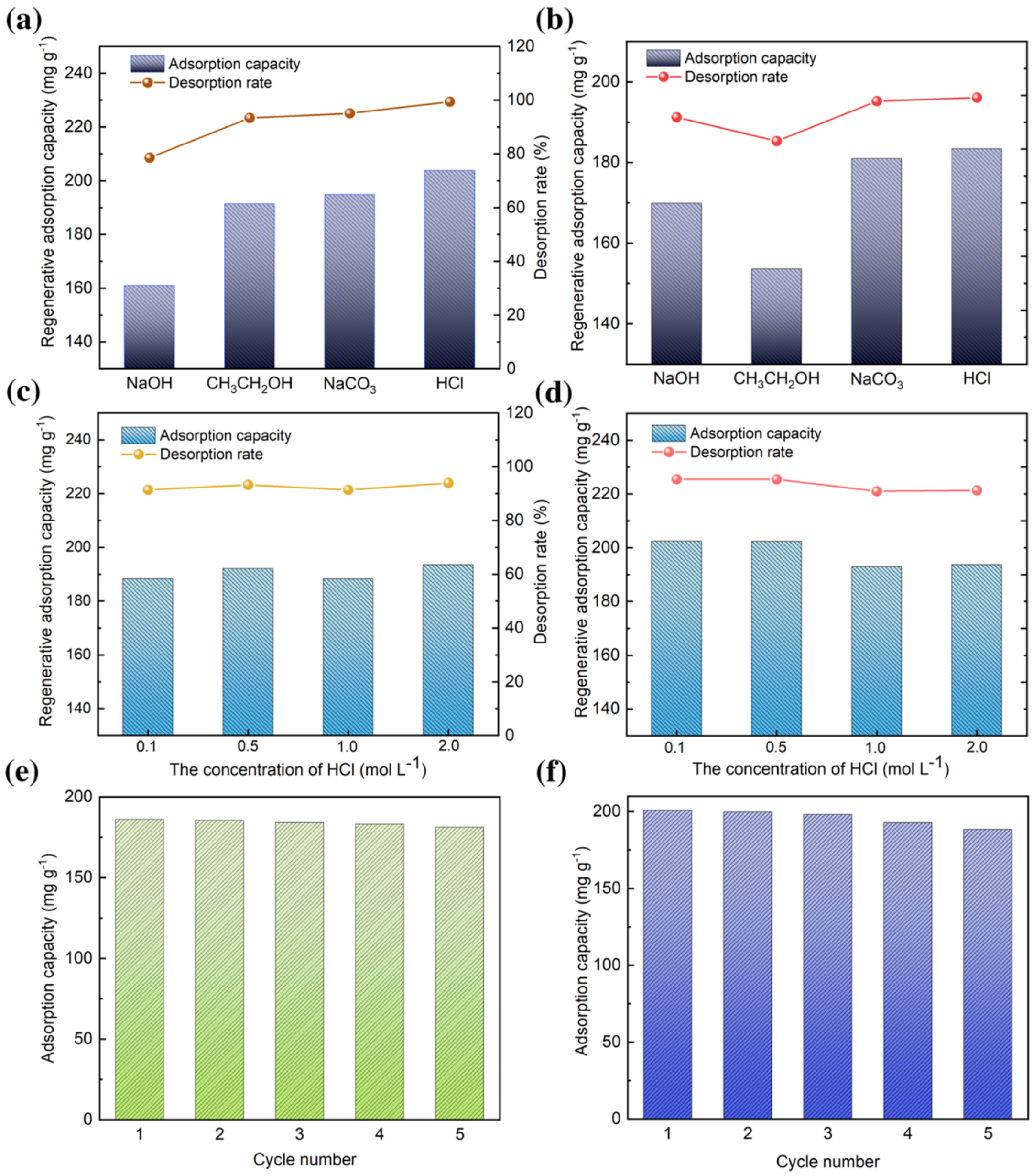

Figure 5. Effect of different desorption agents on CF-PEI desorption: (a) soap yellow; (b) acid red. Effect of HCl concentration on the desorption rate: (c) soap yellow; (d) acid red. Recycling performance: (e) soap yellow; (f) acid red.

high level (>85%), indicating that the adsorption conditions of CF-PEI are relatively mild, which is conducive to the industrial utilization.

Langmuir and Freundlich adsorption isotherm models were further used to fit the adsorption performance of CF-PEI, and the relevant parameters and formulas obtained are shown in Table S1. The curves and linear fitting figures are shown in Figures 3d,e and S10, respectively. By analyzing the fitting results, it can be seen that the Langmuir adsorption isotherm model has a significantly higher fitting degree to the curve than the Freundlich model. Combined with Table S1, the R^2 value of the Langmuir model is all greater than 0.99 at the three temperatures, while that obtained by the Freundlich adsorption isotherm model was lower. Therefore, Langmuir model is more suitable to describe the adsorption process of acid red and soap yellow by CF-PEI. In addition, according to the adsorption strength coefficient n in Table S1, the n values of CF-PEI for acid red and soap yellow are both greater than 1 ($1/n < 1$), indicating that adsorption is easy to occur, and acid red and soap yellow are easy to be adsorbed by CF-PEI.

The thermodynamic study of CF-PEI on the adsorption of soap yellow and acid red is explored by formulating the Gibbs free energy (ΔG), enthalpy change (ΔH), and entropy change (ΔS) of the adsorption reaction process. Related thermodynamic parameters are shown in Table S2. At temperatures of 298, 308, and 318 K, $\Delta G < 0$ indicates that the adsorption of acid red and soap yellow by CF-PEI can proceed spontaneously, and the adsorbate is easily adsorbed on the surface of the adsorbent. In the adsorption of acid red by CF-PEI, $\Delta H < 0$ indicates that the adsorption process is an exothermic reaction, and the increase in temperature is not conducive to the progress of the adsorption process. In the adsorption of soap yellow by CF-PEI, $\Delta H > 0$ indicates that the adsorption process is an endothermic reaction, and the increase in temperature is conducive to the progress of the adsorption process. In the adsorption of CF-PEI to soap

https://doi.org/10.1021/acsomega.1c03643
ACS Omega 2021, 6, 27070−27079

yellow, $\Delta S > 0$ indicates that the entire adsorption process is a more chaotic entropy driving process of the molecular motion at the solid/liquid interface. In the adsorption of acid red by CF-PEI, $\Delta S < 0$ indicates that the entire adsorption process makes the molecular motion at the solid/liquid interface tend to be regular, which is not conducive to adsorption.

Figure 4a,b shows the influence of different adsorption times on the adsorption of simulated dye wastewater by CF-PEI. The adsorption process of soap yellow and acid red by CF-PEI with time can be divided into two stages. During the first 50 min of the adsorption reaction, the adsorption removal rate and equilibrium adsorption capacity increased rapidly, indicating that the adsorption process was a rapid adsorption process. At this stage, there are many vacant adsorption sites on the surface of CF-PEI, and the concentration difference between the surface of the initial adsorbents and the solution is large. The dye molecules in the solution are adsorbed when they collide with each other, and the adsorption rate is fast. When the adsorption time exceeded 50 min, the removal rate and adsorption capacity increased slowly, indicating that the process was a slow adsorption process. At this time, the adsorption sites on the surface of CF-PEI have been gradually filled, the probability of dye molecules in the solution to encounter vacant sites in the contact process decreases, and the concentration gradient of the solution also decreases, leading to the slowdown of the adsorption rate. After adsorption for 60 min, according to the measured data and curve trend, the removal rate and adsorption capacity tended to balance, and the adsorption capacity and removal rate of CF-PEI for soap yellow and acid red were close to the maximum value, which were 206.8 mg g^{-1} and 98.3%, respectively, and 206.8 mg g^{-1} and 99.0%, respectively. Then, the adsorption capacity and removal rate were almost unchanged. At this point, the adsorption reaches saturation. Therefore, the adsorption time can be selected as 100 min in subsequent experiments. Further analysis was made by kinetic equation fitting. The fitting results are shown in Table S3 and Figure 4c,d. The R^2 value of the pseudo-second-order kinetic equation is closer to 1 (0.999 for acid red and 0.998 for soap yellow) compared with that of the pseudo-first-order equation (0.992 for acid red and 0.993 for soap yellow). The adsorption kinetics of the dye by CF-PEI is more suitable to be fitted by the pseudo-second-order kinetics equation. Compared to the previous literature of CF dye absorption material, CF-PEI showed high adsorption capacity and fast adsorption rate, as shown in Table S4.

3.4. Desorption Performance. Desorption and regeneration performance of adsorbents is one of the important properties of adsorbents. In the practical application of adsorbents, the regeneration potential is of great practical significance to reduce the overall treatment cost, and the selection of the appropriate desorbent and the determination of a reasonable concentration of the desorbent are very necessary to realize the regeneration and reuse of adsorbents in practical applications. NaOH, HCl, Na_2CO_3, and CH_5OH were used as desorption agents to regenerate CF-PEI adsorbent after adsorption of soap yellow and acid red. The desorption effects of four different desorbents on saturated CF-PEI are shown in Figure 5a,b. HCl showed the best desorption effect on CF-PEI saturated with soap yellow and acid red, with the highest desorption rates of 99.41% (soap yellow) and 99.16% (acid red), respectively. The desorption effect of NaOH solution and Na_2CO_3 solution on soap yellow was relatively good, while the desorption effect of CH_5OH was relatively poor. The desorption effect of Na_2CO_3 solution on acid red was relatively better, followed by NaOH, and that of CH_5OH was the worst. Therefore, HCl was selected as the desorption agent in subsequent experiments. As shown in Figure 5c,d, the increase of HCl concentration from 0.1 to 2 mol L^{-1} had a limited effect on the desorption of CF-PEI saturated with soap yellow and acid red, and the desorption rates fluctuated above 90%. In general, only 0.1 mol L^{-1} HCl is needed for the desorption of CF-PEI saturated with soap yellow and acid red to achieve a good desorption effect. As shown in Figure 5e,f, the adsorption capacity of saturated CF-PEI on soap yellow only slightly decreased after five cycles of regeneration, gradually decreasing from 186.1 to 181.2 mg g^{-1}. The adsorption capacity of acid red also decreased little and remained 188.5 mg g^{-1} after five cycles. It can be seen that CF-PEI still has a good adsorption effect after five cycles, and the use cost can be reduced by recycling CF-PEI.

3. CONCLUSIONS

CF was used as the matrix, glutaraldehyde was used as the cross-linking agent, and ammoniating modifier was used to prepare the cationic modified CF with good adsorption performance for anionic dyes, which greatly improves the adsorption performance of CFs and further creates conditions for the recycling of waste leather produced by the leather manufacturing industry. Three kinds of ammoniating agents, including triethylenetetramine (TETA), tetraethylenepentamine (TEPA), and PEI, were selected to modify the CF. The results showed that the adsorption capacity of CF modified by three kinds of ammoniating agents on anionic dyes had been greatly improved, among which PEI had the best modification effect. The characterization and physical and chemical properties of CF-PEI showed that the original fibrous structure of CF-PEI was still maintained, and thus the reaction and adsorption area of CF-PEI was larger. The content of primary amino on CF-PEI increased significantly, which not only improved the hydrophilic swelling property of CF but also improved the adsorption property of anionic dye molecules. Studies on the adsorption properties of soap yellow and acid red by CF-PEI showed that in a certain range of acid to neutral, CF-PEI was favorable for the adsorption of anionic dye wastewater. The adsorption isotherm, adsorption thermodynamics, and kinetics analysis showed that the Langmuir adsorption isotherm model was more suitable for CF-PEI adsorption of soap yellow and acid red than the Freundlich model. The adsorption of soap yellow and acid red by CF-PEI can be carried out spontaneously, and the adsorbents are easy to be adsorbed on the surface of the adsorbent. CF-PEI can be desorbed well by a dilute concentration of HCl, and CF-PEI has excellent recycling performance. In this paper, a simple and mild modification method was adopted to improve the adsorption performance of waste leather produced by leather manufacturing industry to common anionic dye wastewater and further expand the idea for the recycling of waste leather produced by leather manufacturing industry.

4. MATERIALS AND METHODS

4.1. Chemical Reagents. CFs prepared from cattle hide were provided by National Engineering Laboratory for Clean Technology of Leather Manufacture. Next, the samples obtained from previous step were dehydrated with anhydrous ethanol, and CFs with a particle size less than 1.0 mm were

https://doi.org/10.1021/acsomega.1c03643
ACS Omega 2021, 6, 27070−27079

formed by crushing and screening. PEI (M.W. 600, 99%), soap yellow, acid red, and glutaraldehyde were provided by Shanghai Aladdin Biotechnology Co. Ltd. (Shanghai, China). TETA, TEPA, NaOH, CH_5OH, Na_2CO_3, and HCl were provided by Sinopharm Chemical Reagent Co. Ltd. All chemicals and reagents used in this study are of analytical reagent grade. Table 1 shows the basic information about the chemicals used in the experiment.

Table 1. CAS Registry Number and Mass Fraction Purity of the Chemicals

component	CAS Reg. no.	suppliers	mass fraction
PEI	9002-98-6	Shanghai Aladdin Biotechnology Co., Ltd.	≥0.990
TETA	112-24-3	Sinopharm Chemical Reagent Co. Ltd.	≥0.990
TEPA	112-57-2	Sinopharm Chemical Reagent Co. Ltd.	≥0.990
soap yellow	587-98-4	Shanghai Aladdin Biotechnology Co. Ltd.	≥0.990
acid red	25641-18-3	Shanghai Aladdin Biotechnology Co. Ltd.	≥0.990
glutaraldehyde	111-30-8	Shanghai Aladdin Biotechnology Co. Ltd.	=0.500
NaOH	1310-73-2	Sinopharm Chemical Reagent Co. Ltd.	≥0.990
CH_5OH	64-17-5	Sinopharm Chemical Reagent Co. Ltd.	≥0.990
Na_2CO_3	497-19-8	Sinopharm Chemical Reagent Co. Ltd.	≥0.990
HCl	7647-01-0	Sinopharm Chemical Reagent Co. Ltd.	0.360–0.380

4.2. Preparation of Cationic CFs. Three kinds of ammoniating agents, TETA, TEPA, and PEI, were used for cationic modification of skin CFs. First, an ammoniator with the same mass as the CF was dissolved in deionized water (deionized water: CF = 50:1 v/w), and then a glutaraldehyde solution with a mass concentration of 3% was prepared (solution volume: CF mass = 50:1). The CF was placed in a three-necked flask for the stirring reaction, and ammonia solution and glutaraldehyde solution were dropped into the three-necked flask at the same time. After the reagent was added, the reaction was carried out at 308 K for 12 h. Then, they were washed with anhydrous ethanol and deionized water separately. After drying and grinding, the cationic CFs including CF-TETA, CF-TEPA, and CF-PEI were obtained (Scheme 2).

4.3. Characterization. The microstructure of the synthesized samples was observed by field emission scanning electron microscopy (FESEM, Nova NanoSEM 230, FEI, USA). The functional groups of the samples were analyzed by FT-IR spectroscopy (AVAT-AR 360, Nicolet, USA) and XPS (ESCALAB 250, ThermoFisher, USA).

4.4. Adsorption Experiments. Three kinds of modified CFs (0.05 g each) were used to oscillate and adsorb 100 mL of 100 mg L^{-1} soap yellow solution and acid red solution for 12 h, and the adsorption capacity was calculated. By analyzing the adsorption capacity of soap yellow and acid red, the CFs modified by the three different ammoniating agents were selected.

In order to discuss the effect of different pH values on adsorption performance, NaOH and HCl (both at the concentration of 0.1 mol L^{-1}) were used to adjust the pH value (2−12) of the system. The conical flask was put into a constant temperature oscillating bed, and the conical flask was oscillated at a constant temperature of 298 K and a rotation speed of 150 r min^{-1} for 12 h.

The adsorption isotherm was studied by the adsorption equilibrium experiment of various soap yellow and acid red concentrations (50.0−400.0 mg L^{-1}) with 50 mL at different temperatures (298, 308, and 318 K). The dosage of the CF-PEI adsorbent was 0.025 g. For the adsorption kinetics, the soap yellow and acid red solutions with an initial concentration of 100.0 mg L^{-1} with 200 mL was adsorbed at 298 K, and the remaining concentration was monitored at intervals. The dosage of the CF-PEI adsorbent was 0.1 g. The residual soap yellow and acid red concentrations in the solution were determined by an UV-vis spectrophotometer (UV-1780, Shimadzu, Japan) at 444 and 516 nm, respectively.

4.5. Desorption Experiments. The adsorption−desorption experiment was used to evaluate the regeneration performance of the cationized CF adsorbent. NaOH, HCl, Na_2CO_3, and CH_5OH were used as desorption adsorbents to regenerate the two dyes. After adsorption, 0.025 g of CF-PEI saturated with dye adsorption was washed with deionized water and then placed in 50 mL of 1 mol L^{-1} desorption solution. The solution was resolved by oscillation at 298 K for 12 h. After desorption, the concentration of soap yellow and acid red in the solution was measured by an UV−vis spectrophotometer, and the desorption rate and adsorption

Scheme 2. Scheme of the Preparation Process of Cationic CFs

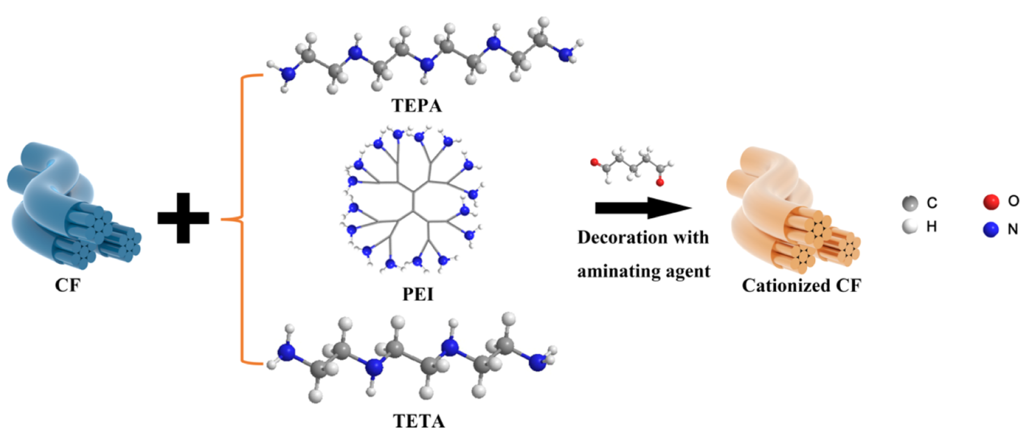

https://doi.org/10.1021/acsomega.1c03643
ACS Omega 2021, 6, 27070−27079

capacity were calculated. The effect of desorption concentration on the desorption efficiency was also investigated. Similar to the desorption selection experiment, 50 mL of HCl desorption solution with concentrations of 0.1, 0.5, 1‾, and 2 mol L^{-1} were used for desorption of 0.05 g of CF-PEI.

■ ASSOCIATED CONTENT

Supporting Information

The Supporting Information is available free of charge at https://pubs.acs.org/doi/10.1021/acsomega.1c03643.

Schematic diagram of ammoniated CF synthesis, adsorption capacity at different reaction temperatures, effect of different ammoniator to CF mass ratios on the adsorption performance of CF-PEI, FESEM images of the CF, high-resolution XPS spectra of the CF and CF-PEI, zeta potential curves of CF-PEI and CF, optical microscope images of the CF and CF-PEI, optical microscope images of the swelling behavior of CF and CF-PEI, effect of solution pH on adsorption soap yellow and acid red, high-resolution XPS spectra of the CF-PEI and CF-PEI after adsorbing soap yellow and acid red, isotherms of soap yellow and acid red adsorbed on CF-PEI fitted by the Freundlich equation, Langmuir and Freundlich adsorption fitting parameters for acid red and soap yellow adsorbed by CF-PEI, thermodynamic parameters of soap yellow and acid red adsorbed by CF-PEI, adsorption kinetics of acid red and soap yellow adsorbed by CF-PEI, and comparison of dye adsorption between the present adsorbent and other adsorbents (PDF)

■ AUTHOR INFORMATION

Corresponding Authors

Xiaoxia Ye − *Fujian Provincial Engineering Research Center of Rural Waste Recycling Technology, College of Environment & Safety Engineering, Fuzhou University, Minhou, Fujian 350108, PR China*; Email: yexiaoxia@fzu.edu.cn

Jie Chen − *College of Environment & Safety Engineering, Fuzhou University, Minhou, Fujian 350108, PR China;* orcid.org/0000-0003-0724-6911; Email: jiechen@fzu.edu.cn

Authors

Wei Luo − *Fujian Provincial Engineering Research Center of Rural Waste Recycling Technology, College of Environment & Safety Engineering, Fuzhou University, Minhou, Fujian 350108, PR China;* orcid.org/0000-0002-2332-701X

Ruiyang Chi − *Fujian Provincial Engineering Research Center of Rural Waste Recycling Technology, College of Environment & Safety Engineering, Fuzhou University, Minhou, Fujian 350108, PR China*

Fanke Zeng − *Fujian Provincial Engineering Research Center of Rural Waste Recycling Technology, College of Environment & Safety Engineering, Fuzhou University, Minhou, Fujian 350108, PR China*

Yahan Wu − *Fujian Provincial Engineering Research Center of Rural Waste Recycling Technology, College of Environment & Safety Engineering, Fuzhou University, Minhou, Fujian 350108, PR China*

Yun Chen − *Fujian Provincial Engineering Research Center of Rural Waste Recycling Technology, College of Environment & Safety Engineering, Fuzhou University, Minhou, Fujian 350108, PR China*

Shuting Liu − *Fujian Provincial Engineering Research Center of Rural Waste Recycling Technology, College of Environment & Safety Engineering, Fuzhou University, Minhou, Fujian 350108, PR China*

Wei Lin − *Fujian Provincial Engineering Research Center of Rural Waste Recycling Technology, College of Environment & Safety Engineering, Fuzhou University, Minhou, Fujian 350108, PR China*

Huiting Lin − *Fujian Provincial Engineering Research Center of Rural Waste Recycling Technology, College of Environment & Safety Engineering, Fuzhou University, Minhou, Fujian 350108, PR China*

Complete contact information is available at: https://pubs.acs.org/10.1021/acsomega.1c03643

Notes

The authors declare no competing financial interest.

■ ACKNOWLEDGMENTS

This research was financially supported by the National Natural Science Foundation of China (no. 22008035), Fujian Industry-University-Research Project (no. 2019H6008), the Natural Science Foundation of Fujian Province, China (no. 2020J05131), the Science and Technology Project of Fujian Educational Committee (no. JAT190053) and the Research Initiation Funding of Fuzhou University (no. GXRC-19060).

■ REFERENCES

(1) Wan Ngah, W. S.; Teong, L. C.; Hanafiah, M. A. K. M. Adsorption of Dyes and Heavy Metal Ions by Chitosan Composites: A Review. *Carbohydr. Polym.* **2011**, *83*, 1446−1456.

(2) Molavi, H.; Shojaei, A.; Pourghaderi, A. Rapid and Tunable Selective Adsorption of Dyes Using Thermally Oxidized Nanodiamond. *J. Colloid Interface Sci.* **2018**, *524*, 52−64.

(3) El Haddad, M.; Regti, A.; Laamari, M. R.; Slimani, R.; Mamouni, R.; Antri, S. E.; Lazar, S. Calcined Mussel Shells as a New and Eco-Friendly Biosorbent to Remove Textile Dyes from Aqueous Solutions. *J. Taiwan Inst. Chem. Eng.* **2014**, *45*, 533−540.

(4) Zhang, Y.; Wan, H.; Zhao, J.; Li, J. Biosorption of Anionic and Cationic Dyes via Raw and Chitosan Oligosaccharide-Modified Huai Flos Chrysanthemum at Different Temperatures. *RSC Adv.* **2019**, *9*, 11202−11211.

(5) An, Y.; Zheng, H.; Zheng, X.; Sun, Q.; Zhou, Y. Use of a Floating Adsorbent to Remove Dyes from Water: A Novel Efficient Surface Separation Method. *J. Hazard. Mater.* **2019**, *375*, 138−148.

(6) Lin, J.; Zhang, Y.; Zhang, Q.; Shang, J.; Deng, F. Enhanced Adsorption Properties of Organic ZnCr-LDH Synthesized by Soft Template Method for Anionic Dyes. *Environ. Sci. Pollut. Res.* **2021**, *28*, 48236.

(7) Zhao, D.; Cai, C. Cerium-Based UiO-66 Metal-Organic Framework for Synergistic Dye Adsorption and Photodegradation: A Discussion of the Mechanism. *Dyes Pigm.* **2021**, *185*, 108957.

(8) Paredes-Quevedo, L. C.; González-Caicedo, C.; Torres-Luna, J. A.; Carriazo, J. G. Removal of a Textile Azo-Dye (Basic Red 46) in Water by Efficient Adsorption on a Natural Clay. *Water, Air, Soil Pollut.* **2021**, *232*, 4.

(9) Chen, K.; Feng, Q.; Ma, D.; Huang, X. Hydroxyl Modification of Silica Aerogel: An Effective Adsorbent for Cationic and Anionic Dyes. *Colloids Surf., A* **2021**, *616*, 126331.

(10) Silva, L. S.; Ferreira, F. J. L.; Silva, M. S.; Citó, A. M. G. L.; Meneguin, A. B.; Sábio, R. M.; Barud, H. S.; Bezerra, R. D. S.; Osajima, J. A.; Silva Filho, E. C. Potential of Amino-Functionalized Cellulose as an Alternative Sorbent Intended to Remove Anionic

Dyes from Aqueous Solutions. *Int. J. Biol. Macromol.* **2018**, *116*, 1282−1295.
(11) Chukwuemeka-Okorie, H. O.; Ekuma, F. K.; Akpomie, K. G.; Nnaji, J. C.; Okereafor, A. G. Adsorption of Tartrazine and Sunset Yellow Anionic Dyes onto Activated Carbon Derived from Cassava Sievate Biomass. *Appl. Water Sci.* **2021**, *11*, 27.
(12) Foo, K. Y.; Hameed, B. H. Microwave Assisted Preparation of Activated Carbon from Pomelo Skin for the Removal of Anionic and Cationic Dyes. *Chem. Eng. J.* **2011**, *173*, 385−390.
(13) Demirbas, A. Agricultural Based Activated Carbons for the Removal of Dyes from Aqueous Solutions: A Review. *J. Hazard. Mater.* **2009**, *167*, 1−9.
(14) Al-Degs, Y. S.; El-Barghouthi, M.; El-Sheikh, A.; Walker, G. Effect of Solution PH, Ionic Strength, and Temperature on Adsorption Behavior of Reactive Dyes on Activated Carbon. *Dyes Pigm.* **2008**, *77*, 16−23.
(15) Greluk, M.; Hubicki, Z. Evaluation of Polystyrene Anion Exchange Resin for Removal of Reactive Dyes from Aqueous Solutions. *Chem. Eng. Res. Des.* **2013**, *91*, 1343−1351.
(16) Chen, J.; Jiang, M.; Han, J.; Liu, K.; Liu, M.; Wu, Q. Syntheses of Magnetic GO @ Melamine Formaldehyde Resin for Dyes Adsorption. *Mater. Res. Express* **2019**, *6*, 086103.
(17) Zheng, J.; Du, L.; Gao, P.; Chen, K.; Ma, L.; Liu, Y.; You, S. Mino-Modified Biomass for Highly Efficient Removal of Anionic Dyes from Aqueous Solutions. *J. Taiwan Inst. Chem. Eng.* **2021**, *119*, 136−145.
(18) Abdulrazzaq, N. N.; Al-Sabbagh, B. H.; Shanshool, H. A. Coupling of Electrocoagulation and Microflotation for the Removal of Textile Dyes from Aqueous Solutions. *J. Water Process Eng.* **2021**, *40*, 101906.
(19) Sathish, M.; Madhan, B.; Raghava Rao, J. Leather solid waste: An eco-benign raw material for leather chemical preparation - A circular economy example. *Waste Manage.* **2019**, *87*, 357−367.
(20) Santos, R. J.; Agostini, D. L. S.; Cabrera, F. C.; Budemberg, E. R.; Job, A. E. Recycling Leather Waste: Preparing and Studying on the Microstructure, Mechanical, and Rheological Properties of Leather Waste/Rubber Composite. *Polym. Compos.* **2015**, *36*, 2275−2281.
(21) Ramesh, R. R.; Muralidharan, V.; Palanivel, S. Preparation and application of unhairing enzyme using solid wastes from the leather industry-an attempt toward internalization of solid wastes within the leather industry. *Environ. Sci. Pollut. Res.* **2018**, *25*, 2121−2136.
(22) Zhu, H.; Wang, B.; Zhu, W.; Duan, T.; He, G.; Wei, Y.; Sun, D.; Zhou, J. Space and Structure Activation of Collagen Fiber for High Efficient Capture Iodine in Off-Gas. *Colloids Surf., A* **2021**, *617*, 126389.
(23) Jing, X.; Li, X.; Jiang, Y.; Zhao, R.; Ding, Q.; Han, W. Excellent Coating of Collagen Fiber/Chitosan-Based Materials That Is Water- and Oil-Resistant and Fluorine-Free. *Carbohydr. Polym.* **2021**, *266*, 118173.
(24) Liao, X.-p.; Shi, B. Adsorption of Fluoride on Zirconium(IV)-Impregnated Collagen Fiber. *Environ. Sci. Technol.* **2005**, *39*, 4628−4632.
(25) Liao, X.; Lu, Z.; Du, X.; Liu, X.; Shi, B. Collagen Fiber Immobilized Myrica Rubra Tannin and Its Adsorption to UO_2^{2+}. *Environ. Sci. Technol.* **2004**, *38*, 324.
(26) Martin, R. B.; Ishida, J. The Relative Effects of Collagen Fiber Orientation, Porosity, Density, and Mineralization on Bone Strength. *J. Biomech.* **1989**, *22*, 419−426.
(27) Doillon, C. J.; Dunn, M. G.; Bender, E.; Silver, F. H. Collagen Fiber Formation in Repair Tissue: Development of Strength and Toughness. *Collagen Relat. Res.* **1985**, *5*, 481−492.
(28) Weadock, K. S.; Miller, E. J.; Keuffel, E. L.; Dunn, M. G. Effect of Physical Crosslinking Methods on Collagen-Fiber Durability in Proteolytic Solutions. *J. Biomed. Mater. Res.* **1996**, *32*, 221−226.
(29) Deng, D.; Liao, X.; Liu, X.; Shi, B. Synthesis of Hierarchical Mesoporous Zirconia Fiber by Using Collagen Fiber as a Template. *J. Mater. Res.* **2008**, *23*, 3263−3268.
(30) Wang, W.; Liu, Y.; Liu, A.; Zhao, Y.; Chen, X. Effect of in Situ Apatite on Performance of Collagen Fiber Film for Food Packaging Applications. *J. Appl. Polym. Sci.* **2016**, *133*, 44154.
(31) Eklouh-Molinier, C.; Happillon, T.; Bouland, N.; Fichel, C.; Diébold, M.-D.; Angiboust, J.-F.; Manfait, M.; Brassart-Pasco, S.; Piot, O. Investigating the Relationship between Changes in Collagen Fiber Orientation during Skin Aging and Collagen/Water Interactions by Polarized-FTIR Microimaging. *Analyst* **2015**, *140*, 6260−6268.
(32) Tovar, N.; Murthy, N. S.; Kohn, J.; Gatt, C.; Dunn, M. ACL Reconstruction Using a Novel Hybrid Scaffold Composed of Polyarylate Fibers and Collagen Fibers. *J. Biomed. Mater. Res., Part A* **2012**, *100A*, 2913−2920.
(33) Huang, W.-Y.; Hibino, T.; Suye, S.-i.; Fujita, S. Electrospun collagen core/poly-l-lactic acid shell nanofibers for prolonged release of hydrophilic drug. *RSC Adv.* **2021**, *11*, 5703−5711.
(34) He, N.; Ke, Q.; Huang, C.; Yang, J.; Guo, Y. Needle-Punched Nonwoven Matrix from Regenerated Collagen Fiber for Cartilage Tissue Engineering. *J. Appl. Polym. Sci.* **2014**, *131*, 40404.
(35) Liu, Y.; Huang, X.; Guo, P.; Liao, X.; Shi, B. Skin Collagen Fiber-Based Radar Absorbing Materials. *Chin. Sci. Bull.* **2011**, *56*, 202−208.
(36) Liao, X.; Zhang, M.; Shi, B. Collagen-Fiber-Immobilized Tannins and Their Adsorption of Au(III). *Ind. Eng. Chem. Res.* **2004**, *43*, 2222−2227.
(37) Liao, X.-P.; Tang, W.; Zhou, R.-Q.; Shi, B. Adsorption of Metal Anions of Vanadium(V) and Chromium(VI) on Zr(IV)-Impregnated Collagen Fiber. *Adsorption* **2008**, *14*, 55−64.
(38) Li, S.; Wang, Y.; Xu, W.; Shi, B. Natural Rubber-Based Elastomer Reinforced by Chemically Modified Multiscale Leather Collagen Fibers with Excellent Toughness. *ACS Sustainable Chem. Eng.* **2020**, *8*, 5091−5099.
(39) Lee, W.; Moghaddam, A. O.; Lin, Z.; McFarlin, B. L.; Wagoner Johnson, A. J.; Toussaint, K. C. Quantitative Classification of 3D Collagen Fiber Organization From Volumetric Images. *IEEE Trans. Med. Imaging* **2020**, *39*, 4425−4435.
(40) Kimura-Suda, H.; Nakamura, F.; Oseto, R.; Kanehira, Y.; Sato, D.; Fujita, R.; Ota, M.; Takahata, M. Relationships among Collagen Fiber Orientation, Mineralization, Mineral Maturity, and Crystallinity. *Mol. Cryst. Liq. Cryst.* **2020**, *707*, 154−160.

https://doi.org/10.1021/acsomega.1c03643
ACS Omega 2021, 6, 27070−27079